

Optical spectroscopy of SmN: Locating the 4*f* conduction band

W. F. Holmes-Hewett,¹ R. G. Buckley,² B. J. Ruck,¹ F. Natali,¹ and H. J. Trodahl¹

¹*MacDiarmid Institute for Advanced Materials and Nanotechnology and School of Chemical and Physical Sciences, Victoria University of Wellington, P.O. Box 600, Wellington 6140, New Zealand*

²*MacDiarmid Institute for Advanced Materials and Nanotechnology and Robinson Research Institute, Victoria University of Wellington, P.O. Box 600, Wellington 6140, New Zealand*



(Received 20 March 2019; revised manuscript received 19 April 2019; published 20 May 2019)

The rare-earth nitride ferromagnetic semiconductors owe their varying magnetic properties to the progressive filling of the 4*f* shell across the series. Recent electrical transport measurements on samarium nitride, including the observation of superconductivity, have been understood in terms of a contribution from a 4*f* transport channel. Band structure calculations generally locate an empty majority-spin 4*f* band within the conduction band although over a wide range of possible energies. Here we report optical reflection and transmission measurements on samarium nitride from 0.01 to 4 eV that demonstrate clearly that the 4*f* band forms the bottom of the conduction band. Results at the lowest energies show no free carrier absorption, indicating a semiconducting ground state, and support earlier conclusions based on transport measurements.

DOI: [10.1103/PhysRevB.99.205131](https://doi.org/10.1103/PhysRevB.99.205131)

I. INTRODUCTION

The remarkable behaviors precipitated by electron correlations in condensed matter systems determines that they have developed an intense interest within the solid-state physics community [1–3]. Within that literature the most striking and most potentially exploitable behavior occurs when a very narrow, high-mass, strongly localized band with a large density of states crosses and hybridizes with a conventional conduction band [4,5]. There is, however, a paucity of simple systems displaying strongly correlated electron characteristics. Within this picture the LN series (L a lanthanide element) shows promise as a valuable testing ground for simply structured, strongly correlated materials due to their rock-salt structure and varying occupancy of the 4*f* shell along the series [3,6–8]. Here we report optical spectroscopy which shows that a localized band forms the conduction band minimum in the ferromagnetic semiconductor SmN.

The members of the LN series share the simple NaCl crystal structure with 4*f* bands crossing the 2*p* valence band (VB) or the 5*d* conduction band (CB) at an energy that varies among the 14 members. Most show semiconducting behavior amenable to tuning the Fermi energy into the heavy-mass 4*f* bands with modest doping levels [6,9]. They have widely ranging magnetic behaviors associated with the varying 4*f* configuration, affecting both the quantum state and its interaction with the electron transport bands, and in at least one case, SmN, a superconducting state is found to occur below 4 K [10].

The prototypical LN is GdN [11], which serves as a valuable benchmark to compare with the other members of the series, based in part on the simplicity offered by the half-filled 4*f* shell in the Gd³⁺ ion. GdN shows ferromagnetic alignment below its Curie temperature of ≈ 70 K [12] and a fully spin polarized conduction channel up to doping levels of 10^{21} cm⁻³

[13]. The ⁸S_{7/2} configuration of its 4*f* shell features $L = 0$, $S = J = 7/2$ ensuring that the majority- (minority)-spin 4*f* band lies 7 eV below (5 eV above) the band gap [6,14]. This in turn ensures no strong electron correlation characteristics with the N 2*p* VB and Gd 5*d* CB both of which are well separated from the 4*f* bands. GdN features a VB maximum at Γ and CB minimum at X, as is expected also for the remaining LN.

With two fewer electrons, SmN adopts a ⁶H_{5/2} configuration leaving two unfilled majority-spin 4*f* states. A free Sm³⁺ ion has a Landé *g* factor of $g_J = 2/7$, and a resulting ground-state moment of $\mu_{BGJ} = 0.71 \mu_B$. In the crystal field the paramagnetic state of SmN carries a magnetic moment of $0.45 \mu_B$, falling to $0.035 \mu_B$ under the combined crystal field and exchange interaction below the ≈ 30 K Curie temperature [18,19]. Such a small magnetic moment results from a nearly complete cancellation between opposing spin and orbital contributions in the partially filled 4*f* shell.

The electronic structure of SmN has been investigated within various density functional theory treatments which show the lowest unoccupied majority-spin 4*f* band [6,15–17] to lie variously from the bottom of the 5*d* conduction band to some few eV higher. This is shown in Fig. 1, along with the 5*d* band which forms the CB minimum across many of the LN series. Interestingly none of the predictions place the 4*f* band below the 5*d*, with even the lowest predicted energy leading only to a strong 4*f*/5*d* hybridization near the bottom of the 5*d* band which then repels the main weight of the 5*d* states to higher energy and leaves the potential of a hybridization gap above the 4*f* band. Recent experimental reports of an enhanced anomalous Hall effect [20] and superconductivity [10] in SmN both show some degree of 4*f* influence on the conduction channel, implying that the 4*f* band does indeed exist near, if not form, the CB minimum. Nearly all calculations also result in a semimetallic ground state, in stark contrast to recent experimental reports all of which support

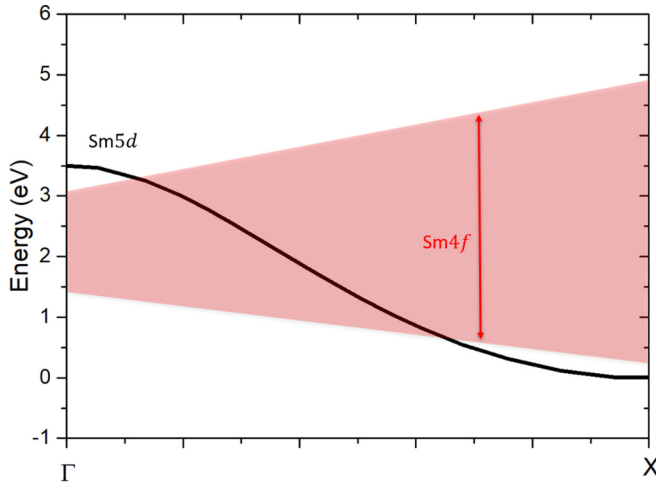


FIG. 1. Schematic band structure diagram showing the range of calculated locations of lowest unoccupied Sm $4f$ majority-spin band (shaded), along with the $5d$ band of SmN for reference (solid black). Plots are scaled such that zero energy is taken at the CB minimum. Data reproduced from Refs. [6,15–17].

the semiconducting conclusion [9,10,18,20,21]. It is clearly important to establish a band structure of SmN and determine the role played by the $4f$ band.

In the present manuscript we inform the calculations with 0.01–4 eV optical spectroscopy delineating these features. We compare measurements on SmN and GdN in the context of their electronic structures and locate the $4f$ band, which we show forms the bottom of the conduction band in SmN.

II. EXPERIMENTAL METHODS

Thin films of SmN and GdN ≈ 100 – 300 nm were grown as detailed in our recent review [9]. Various substrates, suited to each optical or characterisation measurement, were included in each growth to ensure consistency across the various measurements. Films were capped with ≈ 100 nm of AlN for protection from the damaging effects of atmospheric oxygen and water vapor. Electrical measurements were conducted on sapphire [0001] $10 \times 10 \times 0.5$ mm³ substrates with predeposited Au contacts in a van der Pauw configuration. These measurements, conducted in an Oxford Cryogenics close cycle cryostat between 300 and 4 K, showed resistivities increasing rapidly at low temperatures for both SmN and GdN implying low carrier densities and in turn a low concentration of nitrogen vacancies. Reflection and transmission measurements were conducted using a Bruker Vertex 80v Fourier transform spectrometer in which samples were mounted on a cold finger inside an Oxford Cryogenics flow through LHe cryostat. Low energy measurements (0.01–1.2 eV) were conducted on Si substrates where the material is largely transparent, higher energy measurements (0.12–4 eV) were conducted on sapphire substrates for the same reason. Measurements were conducted as a function of temperature, on both substrate materials down to cryogenic temperatures well below the recognized Curie temperatures of SmN (30 K) and GdN (70 K). Reflection measurements

were taken using a 250 nm Al film as reference and data from Ehrenreich [22] to correct the resulting spectrum.

The software package ReFFIT [23], which uses an inherently Kramers-Kronig consistent sum of Lorentzians to represent the dielectric function $\epsilon(\omega)$ of a material, was used to simultaneously reproduce reflection and transmission measurements on both substrate materials. Analysis for any measurement was conducted only over the range of the measurement (e.g., 0.12–4 eV for sapphire). To account for all high energy behavior above the measurement range a constant value ϵ_∞ was first determined by matching the amplitude and phase of the interference fringes in the reflectivity data. Reflection and transmission spectra were reproduced independently for the substrates and capping layers enabling the contribution of the LN layers to be investigated independently, free from interference effects and contributions from the capping layer and substrates. When reproducing the LN layers, Lorentzians with a width of 100 cm⁻¹ were used, these were spaced every 100 cm⁻¹ from 300 cm⁻¹ to $40\,000$ cm⁻¹. Phonon absorption near 250 cm⁻¹ was reproduced using a single Lorentzian. Finally, a zero frequency Drude term was used with parameters constrained to the measured dc resistivity. The resulting dielectric functions were then used to calculate the real part of the optical conductivity $\sigma_1(\omega)$, which is now free from interference and absorption effects from the substrate and capping layer.

III. RESULTS AND DISCUSSION

Before the full analysis of the optical conductivity is considered it is instructive to observe the absorption (1-R-T) in SmN and GdN measured at ambient temperature. This is presented in Fig. 2 which is constructed from low energy measurements on Si and high energy measurements on sapphire substrates. Above ≈ 1.2 eV GdN and SmN show a very similar absorption, with differences in magnitude and structure largely due to film thickness and interference effects. GdN shows very little absorption below 1.3 eV in the transparent region below the minimum optical band gap. SmN shows a strong absorption at these energies (identified with cross-hatching). The most logical explanation for this additional absorption, based upon the electronic structure of these materials, is excitation from the VB into the unfilled majority spin $4f$ band of SmN, not present in GdN. This is now discussed in detail, via the optical conductivity, along with low energy and temperature-dependant measurements.

The optical conductivities $\sigma_1(\omega)$ for GdN and SmN are now shown in Fig. 3. This plot shows similar features to the absorption in Fig. 2, but is free from interference effects and contributions from the capping layer and substrates. We begin by discussing GdN in the interband region where $\sigma_1(\omega)$ increases strongly above 1.3 eV. Extrapolation of the absorption above this edge leads to a band gap of 1.35 eV in the paramagnetic phase at room temperature, dropping to 0.85 eV in the ferromagnetic phase at 7 K (7 K data are shown as the dotted series in Fig. 3). Below ≈ 1 eV, $\sigma_1(\omega)$ falls to zero below the minimum optical band gap.

Turning now to the SmN sample, $\sigma_1(\omega)$ above 1.2 eV is very similar to that of GdN with transposition to lower energy

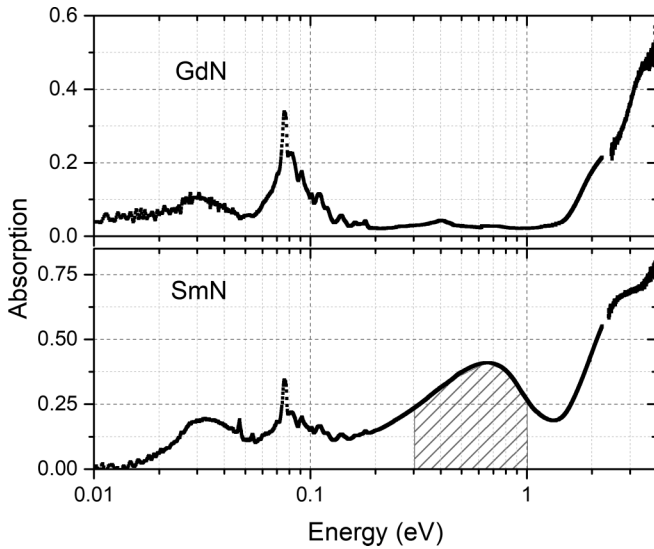


FIG. 2. Measurements of absorption in GdN (top) and SmN (bottom) at ambient temperature. The GdN measurement shows little to no absorption below the fundamental edge at 1.35 eV. The SmN measurement shows a similar absorption beginning above 1.2 eV but in addition a discrete feature at lower energy (identified with cross-hatching) signals additional optical transitions not present in GdN. The features near 0.1 eV shared in both plots are caused by absorption in the Si substrate and AlN capping layer. The broad absorption near 0.03 eV is a phonon absorption in the LN. Differences in magnitude and oscillations at high energy are caused largely by film thickness and interference effects.

on the order of 0.3 eV. Again, extrapolation gives a direct gap for this transition of 1.27 eV in the paramagnetic phase although this is difficult to determine given the overlap with the lower energy feature. We move now to the mid- and near-infrared region spanning 0.1–1 eV. We see no absorption in the GdN below the fundamental edge. Additional absorption is now clearly visible in SmN as illustrated in Fig. 3 by a broad peak in $\sigma_1(\omega)$ centered around 0.5 eV (cross-hatched as in Fig. 2). Not only does this feature indicate absorption at lower energies than for GdN, but also its form reveals information regarding the nature of the band, or density of states, at the bottom of the conduction band.

The task is now to construct a schematic band structure based on the measurements in Fig. 3 and in the context of the calculated band structure of GdN [6,15,24], which is largely consistent with experiment [14,25]. The resulting schematic band structure of SmN is shown in Fig. 4. To begin, the VB must be considered, this is formed from the N 2*p* states as is the case across the semiconducting members of the LN series [6] with the VB maximum at Γ and ≈ 0.5 eV of dispersion before a stationary point at X. The filled 4*f* states, similar to those in GdN, are calculated to be a minimum of ≈ 5 eV below the CB so are of little influence [6]. The 5*d* band which forms the CB minimum in many of the LN, is also qualitatively similar across the series. The data in Fig. 3 show such similarity above 1.2 eV that we propose the absorption here is due to the same 2*p* to 5*d* transition at X that has been so well established in GdN [6,14,25,26]. The feature near 0.5 eV, not present in the GdN data, must then

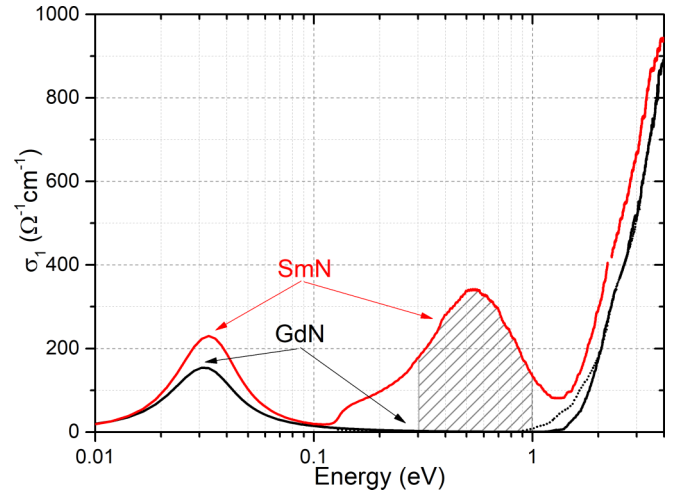


FIG. 3. Real part of the optical conductivity $\sigma_1(\omega)$ based on data visible in Fig. 2 for both SmN (red) and GdN (black) and GdN at 7 K (black dotted). Both materials show a strong increase in $\sigma_1(\omega)$ at high energy due to transitions from the VB to 5*d* bands. The SmN result has an additional feature near 0.5 eV (identified with cross-hatching) which indicates transitions from the VB into a localized 4*f* band, lying below the 5*d*. At the lowest energies a phonon absorption can be seen in each material. At low temperature the ferromagnetic redshift of the optical edge of GdN can be seen. No measurable temperature dependence was seen in measurements of SmN samples.

be described by excitation into some state not present in GdN. The most natural description is then the unfilled majority-spin 4*f* band of SmN implied by both the anomalous Hall effect [20] and superconductivity [10] measurements to be near the CB minimum. The separation of this feature in $\sigma_1(\omega)$ from the absorption at higher energies indicates that optical transitions begin at some point closer to Γ , as the energy of states in the VB increases when moving from X toward the VB maximum at Γ while decreasing monotonically moving from X to W or from X to K.

Figure 4 shows a schematic representation of the band structure of SmN based on measurements in Fig. 3. The 4*f* band is shown with a range of energies for any given wave vector *k* (represented by the shading surrounding the band in the figure) due to its highly localized nature, especially in the case of minimal hybridization. Figure 4 additionally shows the 4*f* band as dispersionless, the width of the 0.5 eV feature in Fig. 3 is then the width of the valance band between Γ and X ≈ 0.5 eV as qualitatively expected from the other LN [6]. Extrapolation from the low energy side of the feature then gives the energy of this band. Figure 4 shows the 1.27 eV gap between the N 2*p* valance band and Sm 5*d* at X in black. The ≈ 0.3 eV minimum optical gap is shown, in the limit of a dispersionless 4*f* band, at the Γ point.

Given the similarities to GdN [14,25] one may expect a temperature-dependant redshift of the optical edge in SmN. To investigate this, temperature-dependant measurements of both reflection and transmission were completed at various temperatures above and below the Curie temperatures of both SmN and GdN. The GdN sample showed a redshift of the optical edge from 1.35 eV in the paramagnetic phase at ambient temperature to 0.85 eV in the ferromagnetic phase at 7 K.

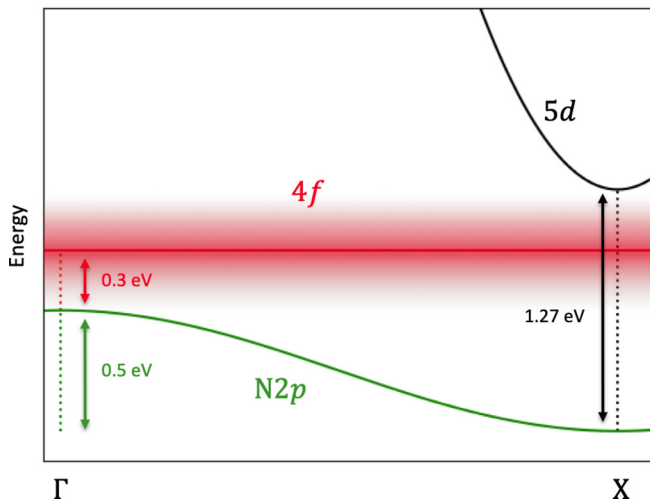


FIG. 4. Schematic band structure for SmN which is consistent with the data in Fig. 3. The Sm $5d$ band, similar to that of GdN, is shown reaching a minimum at the X point, the $N2p$ valence band has its maximum at the Γ point. The Sm $4f$ band, located via measurements shown in Fig. 3, is found beneath the $5d$ and is shown here as dispersionless. Shading is used to represent this as a localized band which lacks a well-defined $\epsilon(k)$ relationship.

The optical conductivity derived from these measurements is visible as the dotted series in Fig. 3. The measured paramagnetic and ferromagnetic gaps in GdN are consistent with previous experimental results [14,25,27,28] showing the reduction of the optical gap in the ferromagnetic phase and calculations [6] which predict a 0.4 eV redshift. Temperature-dependant reflection and transmission measurements on SmN samples showed no change, thus are not shown in Fig. 3. A lack of redshift in the 1.2 eV transition at X is perhaps not so surprising, because any shift would be obscured by the additional absorption at lower energy; this can be seen by considering the magnitude of the redshift of the GdN edge in Fig. 3 and the location of the additional absorption in SmN. The lack of temperature dependence of the 0.5 eV feature is somewhat more surprising, the exchange interaction between the $4f$ electrons below the Curie temperature appears to have very little effect on the optical absorption here.

Previous optical measurements on SmN [29] and NdN [30] films have shown an increase in absorption near 0.5 eV, similar to measurements in the present manuscript. These measurements, however, were not conducted to low enough energy to observe the peak of this feature and as such attributed the increase in absorption to free carriers in conductive films.

Finally, measurements at the lowest energies in Fig. 3 show a phonon absorption in both GdN and SmN at 250 cm^{-1} (31 meV) and 265 cm^{-1} (33 meV) respectively. The measured values are $\approx 20\%$ lower than those predicted [31], as is seen also in DyN [32] and in Raman measurements of several of the LN [31]. As energy approaches zero and the optical conductivity approaches the dc, there is no obvious contribution to $\sigma_1(\omega)$ indicative of absorption from free carriers, this indicates insulating films, consistent with transport measurements and previous experimental results indicating a semiconducting ground state [9,10,18,20,21].

IV. SUMMARY

Optical measurements of reflection and transmission were undertaken on SmN and GdN thin films from ambient to cryogenic temperatures. Measurements on GdN films were consistent with previous reports [14,25,27,28] yielding a band gap of 1.35 eV in the paramagnetic phase reducing to 0.85 eV in the ferromagnetic phase. Measurements on SmN samples above 1.2 eV were very similar to GdN, indicating a transition at X between the VB and Sm $5d$ CB of 1.27 eV. Measurements at lower energies showed additional absorption, not present in GdN, thus indicating a low lying localized $4f$ band, present in the conduction band of SmN but absent in GdN. A schematic band structure diagram of SmN was then created, to be consistent with the present measurements, showing the $4f$ band sitting ≈ 0.3 eV above the VB maximum at Γ , in the limit of a dispersionless $4f$ band. Neither optical edge measured in SmN showed any appreciable shift when cooled below the magnetic transition temperature. In addition measurements down to 0.01 eV revealed phonon absorption in both GdN and SmN at 250 cm^{-1} (31 meV) and 265 cm^{-1} (33 meV) respectively, consistent with theory [31] and optical measurements on DyN [32]. Measurements at the lowest energies showed no indication of free carrier absorption.

The identification of a localized heavy fermion conduction band in SmN provides evidence that the LN series likely harbors several more simply structured strongly correlated materials. The independent control of magnetization, carrier concentration, and scattering rate offered by the semiconducting LN members may now be of interest to both theorists and experimentalists alike, and prove valuable in the investigation of heavy f electron materials.

ACKNOWLEDGMENTS

This research was supported by the New Zealand Marsden Fund (Grants No. 13-VUW1309 and No. 08-VUW-1309). The MacDiarmid Institute is supported under the New Zealand Centres of Research Excellence Programme.

- [1] P. Coleman, Heavy fermions: Electrons at the edge of magnetism, in *Handbook of Magnetism and Advanced Magnetic Materials* (American Cancer Society, Atlanta, 2007).
 [2] L. Degiorgi, *Rev. Mod. Phys.* **71**, 687 (1999).

- [3] R. Adler, C.-J. Kang, C.-H. Yee, and G. Kotliar, *Rep. Prog. Phys.* **82**, 012504 (2018).
 [4] P. S. Riseborough, *Adv. Phys.* **49**, 257 (2000).
 [5] M. Dzero, J. Xia, V. Galitski, and P. Coleman, *Annu. Rev. Condens. Matter Phys.* **7**, 249 (2016).

- [6] P. Larson, W. R. L. Lambrecht, A. Chantis, and M. vanSchilfgaarde, *Phys. Rev. B* **75**, 045114 (2007).
- [7] M. D. Johannes and W. E. Pickett, *Phys. Rev. B* **72**, 195116 (2005).
- [8] C. M. Aerts, P. Strange, M. Horne, W. M. Temmerman, Z. Szotek, and A. Svane, *Phys. Rev. B* **69**, 045115 (2004).
- [9] F. Natali, B. Ruck, N. Plank, H. Trodahl, S. Granville, C. Meyer, and W. Lambrecht, *Prog. Mater. Sci.* **58**, 1316 (2013).
- [10] E.-M. Anton, S. Granville, A. Engel, S. V. Chong, M. Governale, U. Zülicke, A. G. Moghaddam, H. J. Trodahl, F. Natali, S. Vézian, and B. J. Ruck, *Phys. Rev. B* **94**, 024106 (2016).
- [11] S. Granville, B. J. Ruck, F. Budde, A. Koo, D. J. Pringle, F. Kuchler, A. R. H. Preston, D. H. Housden, N. Lund, A. Bittar, G. V. M. Williams, and H. J. Trodahl, *Phys. Rev. B* **73**, 235335 (2006).
- [12] N. O. V. Plank, F. Natali, J. Galipaud, J. H. Richter, M. Simpson, H. J. Trodahl, and B. J. Ruck, *Appl. Phys. Lett.* **98**, 112503 (2011).
- [13] H. J. Trodahl, F. Natali, B. J. Ruck, and W. R. L. Lambrecht, *Phys. Rev. B* **96**, 115309 (2017).
- [14] H. J. Trodahl, A. R. H. Preston, J. Zhong, B. J. Ruck, N. M. Strickland, C. Mitra, and W. R. L. Lambrecht, *Phys. Rev. B* **76**, 085211 (2007).
- [15] T. Cheiwchanchamnangij, Applications of the quasiparticle self-consistent GW method, Ph.D. thesis, Case Western Reserve University, 2014.
- [16] N. N. Som, V. H. Mankad, S. D. Dabhi, A. Patel, and P. K. Jha, *J. Magn. Magn. Mater.* **448**, 186 (2018).
- [17] C. Morari, F. Beiușeanu, I. Di Marco, L. Peters, E. Burzo, S. Mican, and L. Chioncel, *J. Phys. Condens. Matter* **27**, 115503 (2015).
- [18] C. Meyer, B. J. Ruck, J. Zhong, S. Granville, A. R. H. Preston, G. V. M. Williams, and H. J. Trodahl, *Phys. Rev. B* **78**, 174406 (2008).
- [19] J. F. McNulty, B. J. Ruck, and H. J. Trodahl, *Phys. Rev. B* **93**, 054413 (2016).
- [20] W. F. Holmes-Hewett, F. H. Ullstad, B. J. Ruck, F. Natali, and H. J. Trodahl, *Phys. Rev. B* **98**, 235201 (2018).
- [21] E.-M. Anton, B. J. Ruck, C. Meyer, F. Natali, H. Warring, F. Wilhelm, A. Rogalev, V. N. Antonov, and H. J. Trodahl, *Phys. Rev. B* **87**, 134414 (2013).
- [22] H. Ehrenreich, H. R. Philipp, and B. Segall, *Phys. Rev.* **132**, 1918 (1963).
- [23] A. B. Kuzmenko, Guide to REFFIT: Software to fit optical spectra, <http://optics.unige.ch/alexey/refit.html> (2004).
- [24] C. Mitra and W. R. L. Lambrecht, *Phys. Rev. B* **78**, 195203 (2008).
- [25] H. Yoshitomi, S. Kitayama, T. Kita, O. Wada, M. Fujisawa, H. Ohta, and T. Sakurai, *Phys. Rev. B* **83**, 155202 (2011).
- [26] A. R. H. Preston, B. J. Ruck, W. R. L. Lambrecht, L. F. J. Piper, J. E. Downes, K. E. Smith, and H. J. Trodahl, *Appl. Phys. Lett.* **96**, 032101 (2010).
- [27] R. Vidyasagar, T. Kita, T. Sakurai, and H. Ohta, *J. Appl. Phys.* **115**, 203717 (2014).
- [28] M. Azeem, *Chin. Phys. Lett.* **33**, 027501 (2016).
- [29] M. Azeem, *Chin. J. Phys.* **56**, 1925 (2018).
- [30] E.-M. Anton, J. F. McNulty, B. J. Ruck, M. Suzuki, M. Mizumaki, V. N. Antonov, J. W. Quilty, N. Strickland, and H. J. Trodahl, *Phys. Rev. B* **93**, 064431 (2016).
- [31] S. Granville, C. Meyer, A. R. H. Preston, B. M. Ludbrook, B. J. Ruck, H. J. Trodahl, T. R. Paudel, and W. R. L. Lambrecht, *Phys. Rev. B* **79**, 054301 (2009).
- [32] M. Azeem, B. J. Ruck, D. Binh, H. Warring, N. Strickland, A. Koo, V. Goian, S. Kamba, and H. J. Trodahl, *J. Appl. Phys.* **113**, 203509 (2013).